INSTITUTE OF PHYSICS PUBLISHING JOURNAL OF PHYSICS B: ATOMIC, MOLECULAR AND OPTICAL PHYSICS

J. Phys. B: At. Mol. Opt. Phys. **36** (2003) L39–L46 PII: S0953-4075(03)55794-7

LETTER TO THE EDITOR

Converged wavepacket calculations for electron-impact ionization of hydrogen. Comparison with two-electron R-matrix propagation

L Mouret, K M Dunseath, M Terao-Dunseath and J-M Launay

Laboratoire de Physique des Atomes, Lasers, Molécules et Surfaces, UMR 6627 du CNRS-Université de Rennes 1, Campus de Beaulieu, F-35042 Rennes Cedex, France

Received 8 November 2002
Published 20 December 2002
Online at stacks.iop.org/JPhysB/36/L39

Abstract

Total cross sections and asymmetry parameters for electron-impact ionization of hydrogen at intermediate energies are calculated using a wavepacket propagation approach for all partial waves. The time-dependent Schrödinger equation is solved using a grid and a split-operator scheme adapted to the Coulomb potential. The results obtained are in very good agreement with those of experiment and other theoretical approaches, in particular the two-electron R-matrix propagator.

With the widespread availability of powerful computers, it is now feasible to solve directly the time-dependent Schrödinger equation. Such an approach can be easily implemented and presents numerous advantages. A collision can be visualized, which may help us to understand the mechanisms by which various processes occur. The particles may be described by well-localized wavepackets, thus avoiding problems associated with the definition of asymptotic solutions, such as three-body boundary conditions. The use of grid representations also avoids having to evaluate complicated matrix elements. The programs are very flexible and can treat, with relatively minor changes, systems and processes that are apparently very different.

While the time-dependent approach is now widely used in studies of molecular dynamics and laser-assisted processes, its application to atomic collisional processes has been much more limited. Ihra *et al* (1995) developed the pioneering work of Bottcher (1981) to treat electron-impact ionization of hydrogen in the s-wave model. Pindzola and co-workers (Pindzola and Schultz 1996, Pindzola and Robicheaux 1996) applied a time-dependent close-coupling (TDCC) approach to the full scattering system. Their choice of a uniform spatial grid, however, limited their calculations to a small region of configuration space and to the first few partial waves ($L \leqslant 4$). The contribution from higher partial waves was accounted for using a distorted wave method. The method has very recently been extended and used to calculate triple differential cross sections for electron-impact ionization of hydrogen (Colgan *et al* 2002). Pindzola and co-workers have also applied their method to study systems involving more

than two electrons by using frozen core approximations or pseudopotentials (see for example Pindzola and Robicheaux (2000), Pindzola *et al* (2000) and references therein).

Electron–hydrogen scattering is a fundamental benchmark process for which there now exists a wealth of accurate data. In this letter, we report converged results for electron-impact ionization obtained using a wavepacket approach to solve the time-dependent Schrödinger equation. In contrast to the work cited in the previous paragraph, we use a non-uniform spatial grid based on Schwartz interpolation (Schwartz 1985) which is particularly well adapted to describing bound states of the Coulomb potential (Dunseath *et al* (2002), to be referred to as paper I). Our aim here is to demonstrate that this spatial representation is also well adapted to describing two-electron collision systems. In particular, a much larger region of configuration space can be spanned with a reasonable number of points, which allows us to apply the wavepacket propagation method for all partial waves until convergence is achieved. We compare our results with experimental data and also with other accurate theoretical values, in particular those obtained using the two-electron R-matrix propagator (Dunseath *et al* 1996): these are presented here for the first time. Atomic units are used throughout, unless otherwise stated.

The time-dependent Schrödinger equation for electron–hydrogen scattering is

$$H\Psi(\boldsymbol{r}_1, \boldsymbol{r}_2, t) = \mathrm{i}\frac{\partial}{\partial t}\Psi(\boldsymbol{r}_1, \boldsymbol{r}_2, t) \tag{1}$$

where the two-electron Hamiltonian H is given by

$$H = -\frac{1}{2}\nabla_1^2 - \frac{1}{r_1} - \frac{1}{2}\nabla_2^2 - \frac{1}{r_2} + \frac{1}{r_{12}} = h_1 + h_2 + \frac{1}{r_{12}}.$$

Since H is independent of time, the formal solution of equation (1) may be written as

$$\Psi(\boldsymbol{r}_1, \boldsymbol{r}_2, t + \Delta t) = \mathrm{e}^{-\mathrm{i}H\Delta t}\Psi(\boldsymbol{r}_1, \boldsymbol{r}_2, t),$$

which forms the basis of most numerical approaches for propagating the wavefunction in time. We expand the spatial wavefunction for a particular partial wave $\Gamma = \{LMS\Pi\}$ at time t as

$$\Psi^{\Gamma}(\boldsymbol{r}_1, \boldsymbol{r}_2, t) = \sum_{i,j,\ell_1,\ell_2} \alpha^{\Gamma}_{ij\ell_1\ell_2}(t)\psi^{\Gamma}_{ij\ell_1\ell_2}(\boldsymbol{r}_1, \boldsymbol{r}_2) \tag{2}$$

with

$$\psi^{\Gamma}_{ij\ell_1\ell_2}(\boldsymbol{r}_1, \boldsymbol{r}_2) = \frac{1}{r_1 r_2}\varphi_i(r_1)\varphi_j(r_2)\mathcal{Y}^{LM}_{\ell_1\ell_2}(\hat{\boldsymbol{r}}_1, \hat{\boldsymbol{r}}_2) \tag{3}$$

where the $\mathcal{Y}^{LM}_{\ell_1\ell_2}$ are the usual coupled spherical harmonic functions. The main novelty of our approach lies in the choice of the radial functions $\varphi_i(r)$ which are taken to be the cardinal functions of paper I:

$$\varphi_i(r) = \frac{\upsilon(r)}{a_i(r - r_i)}, \tag{4}$$

where r_i is a node of the reference function $\upsilon(r)$ and $a_i = \upsilon'(r_i)$. They have the property

$$\varphi_i(r_j) = \delta_{ij}. \tag{5}$$

Following paper I, we take $\upsilon(r)$ to be the positive-energy Coulomb function $\kappa^{-1/2}F_0(\eta, \kappa r)$, with $\eta = -\mathcal{Z}/\kappa$. The nodes r_i of this function define a non-uniform grid whose distribution can be optimized by varying the parameters $\mathcal{Z}$ and κ. The grid is well adapted for accurately describing the wavefunction over a large portion of configuration space: increasing $\mathcal{Z}$ concentrates more points closer to the origin while the main effect of varying κ is to change the spacing of the points at larger distances. The spatial extent of the grid can also be controlled by the finite number of nodes retained in the calculation. A full description is given in paper I,

where we have shown in particular that a large number of hydrogen bound states can be reproduced very accurately with relatively few points. We have also verified that the full set of states associated with the grid satisfies several sum rules for the radial dipole moments and that the dipole polarizability of the ground state is accurately reproduced, indicating that the grid provides a very good discrete representation of the hydrogen continuum.

The initial wavepacket is taken to be

$$\Psi^{\Gamma}(\boldsymbol{r}_1, \boldsymbol{r}_2, t = 0) = \mathcal{A}_S \frac{1}{r_1 r_2} g_{k_0}(r_1) u_{1s}(r_2) \mathcal{Y}_{L0}^{LM}(\hat{\boldsymbol{r}}_1, \hat{\boldsymbol{r}}_2) \tag{6}$$

where $\mathcal{A}_S$ is the (anti)symmetrization operator. This corresponds to one electron in the hydrogen ground state and an incoming electron described by the Gaussian

$$g_{k_0}(r) = \frac{1}{\pi^{1/4}\sigma_0^{1/2}} \exp\left[-\frac{(r - r_0)^2}{2\sigma_0^2}\right] \exp(-\mathrm{i}k_0 r)$$

where r_0 is the average position, σ_0 is the width and k_0 is the average momentum of the wavepacket. The average kinetic energy is $k_0^2/2 + 1/(4\sigma_0^2)$. The values of the coefficients $\alpha^{\Gamma}_{ij\ell_1\ell_2}(t)$ in equation (2) at time $t = 0$ are determined by the initial wavepacket (6).

To solve the time-dependent Schrödinger equation, we propagate the wavepacket from time $t = 0$ using a split-operator technique (Feit *et al* 1982) adapted to our grid and radial functions (4). We approximate the time-evolution operator by

$$\mathrm{e}^{-\mathrm{i}H\Delta t} = \mathrm{e}^{-\mathrm{i}h_1 \frac{\Delta t}{2}} \mathrm{e}^{-\mathrm{i}h_2 \frac{\Delta t}{2}} \mathrm{e}^{-\mathrm{i}\frac{1}{r_{12}}\Delta t} \mathrm{e}^{-\mathrm{i}h_1 \frac{\Delta t}{2}} \mathrm{e}^{-\mathrm{i}h_2 \frac{\Delta t}{2}} \tag{7}$$

with an error of $\mathcal{O}(\Delta t^3)$. The action of an elementary evolution operator $\exp(-\mathrm{i}\mathcal{H}\Delta t)$ on the wavefunction (2) can be written in matrix form as $\boldsymbol{U}\boldsymbol{\mathcal{E}}\boldsymbol{U}^{\dagger}\boldsymbol{\alpha}$. The diagonal matrix $\boldsymbol{\mathcal{E}}$ has elements $\exp(-\mathrm{i}\varepsilon_i \Delta t)$ where ε_i are the eigenvalues of the operator $\mathcal{H}$, $\boldsymbol{U}$ is the matrix of the associated eigenvectors and $\boldsymbol{\alpha}$ is the vector of coefficients for the wavefunction expanded in basis (3). The matrix representations of $\exp(-\mathrm{i}h_1\Delta t/2)$ and $\exp(-\mathrm{i}h_2\Delta t/2)$ are diagonal in $\{j, \ell_1, \ell_2\}$ and $\{i, \ell_1, \ell_2\}$, respectively. In practice, we therefore diagonalize the one-electron operator h_1 in the basis of cardinal functions (4), h_2 having the same eigenvalues and eigenvectors. The matrix elements of h_1 in this basis are very simple and are given by equation (29) of paper I. The matrix representation of the two-electron operator $1/r_{12}$ is evaluated using its expansion in spherical harmonics. It is block-diagonal by construction in the basis (3) due to the property (5) of the cardinal functions:

$$\left\langle \psi^{\Gamma}_{ij\ell_1\ell_2} \middle| \frac{1}{r_{12}} \middle| \psi^{\Gamma}_{i'j'\ell_1'\ell_2'} \right\rangle = \delta_{ii'}\delta_{jj'} \sum_k \frac{r_<^k}{r_>^{k+1}} \mathcal{K}^{(k)}_{\ell_1\ell_2\ell_1'\ell_2'}$$

with $r_< = \min(r_i, r_j)$, $r_> = \max(r_i, r_j)$ and where $\mathcal{K}^{(k)}_{\ell_1\ell_2\ell_1'\ell_2'}$ are the usual Percival–Seaton coefficients (Percival and Seaton 1957). The action of the time evolution operator (7) on the wavefunction (2) is therefore computed through a series of matrix multiplications.

The probability that after the collision one of the electrons (for example electron 1) is in the exact bound state $|n\ell m\rangle$ of hydrogen is obtained by projecting the wavefunction onto this state and integrating over the coordinates of the other electron:

$$\mathcal{P}^{\Gamma}_{n\ell m}(1) = \int |\langle n\ell m|\Psi^{\Gamma}\rangle_{r_1}|^2 \, \mathrm{d}\boldsymbol{r}_2. \tag{8}$$

The ionization probability is therefore given by

$$\mathcal{P}^{\Gamma}_{\mathrm{I}} = 1 - \sum_{n\ell m} \mathcal{P}^{\Gamma}_{n\ell m}(1) - \sum_{n\ell m} \mathcal{P}^{\Gamma}_{n\ell m}(2) + \sum_{n\ell m} \sum_{n'\ell'm'} |\langle n\ell m, n'\ell'm'|\Psi^{\Gamma}\rangle|^2 \tag{9}$$

where the last term is included to avoid double counting of the contributions from doubly excited states $|n\ell m, n'\ell'm'\rangle$. This procedure is similar to that used by Pindzola and Schultz

(1996) apart from our use of exact hydrogen bound states in the projections in (8) and (9). The total ionization cross section is given by

$$\sigma_{\rm I} = \frac{\pi}{4k_0^2}\sum_{LS\Pi}(2L+1)(2S+1)\mathcal{P}_{\rm I}^{\Gamma}.$$

The probabilities are calculated at sufficiently large times when they have reached a constant value, i.e. the collision is effectively over.

We have used this approach to calculate ionization cross sections for collision energies E from 15 to 40 eV, including all partial waves up to $L = 19$. In order to compare cross sections with those from time-independent calculations at well defined energies, the momentum distribution of the wavepacket must be small, i.e. the width σ_0 of the radial wavepacket must be chosen sufficiently large. The results should then be insensitive to the actual value of σ_0, which we have verified by performing calculations with different widths. The time step Δt is 0.02 au when the wavepacket is close to the nucleus, while at larger distances it is increased to 0.05 au for $E = 15$ eV and to 0.1 au at higher energies. For a fixed collision energy, we calculate the ionization probability at several different times in order to check its convergence and stability. We take the spatial grid sufficiently large to avoid problems associated with reflections on the boundary and thus we do not need to define absorbing potentials. The parameters $\mathcal{Z}$ and κ of the reference function are optimized for each collision energy: $\mathcal{Z}$ generally increases with the collision energy in order to describe the rapidly oscillating wavefunction near the atomic nucleus. At $E = 40$ eV, the size of the grid is 100 a_0 (128 grid points), sufficiently large to reproduce all the hydrogen bound state energies up to $n = 4$ to an accuracy better than 10^{-11} eV. The width σ_0 of the radial wavepacket is taken to be 10 a_0. At $E = 15$ eV, the size of the grid is 320 a_0 (255 grid points), which allows all the hydrogen bound state energies up to $n = 9$ to be reproduced to the same accuracy. The width σ_0 is increased to 30 a_0, so that the energy spread is small relative to the collision energy. The convergence and stability of the results with respect to these parameters have been carefully tested.

In table 1 and figures 1 and 2, we compare the results obtained using the time-dependent approach with those of the two-electron R-matrix propagation method (Dunseath *et al* 1996). In this, the two-electron configuration space is partitioned into elementary domains by dividing the range of each radial coordinate into a number of sectors. The two-electron Hamiltonian is diagonalized in each domain and elementary R-matrices relating the radial functions to their derivatives on the surfaces of the domain are constructed. These are combined with those of neighbouring domains to propagate the global R-matrix in two directions out from $r_e = 0$ to $r_{\rm out}$ ($e = 1, 2$). Target states are defined by diagonalizing the one-electron Hamiltonian in the global sector $[0, r_{\rm out}]$: this yields a discrete set of basis functions of which the lowest correspond very precisely to the first hydrogen bound states, while the others are pseudostates representing highly excited states and the continuum. Beyond $r_{\rm out}$ the scattering problem is solved within the close-coupling formalism using a combination of one-dimensional R-matrix propagation and asymptotic expansion methods. Following Gallaher (1974), the ionization cross section $\sigma_{\rm I}(E)$ at collision energy E is computed as

$$\sigma_{\rm I}(E) = \sum_{\bar{n}}\left(1 - \sum_{n}|\langle n|\bar{n}\rangle|^2\right)\sigma_{\bar{n}}(E)$$

where $\sigma_{\bar{n}}$ is the cross section for excitation into the pseudostate $|\bar{n}\rangle$ and $|n\rangle$ is a physical state of hydrogen. This formula can be interpreted as the difference between the total cross section and the cross section for excitation into the physical bound states. Alternatively, the coefficient multiplying $\sigma_{\bar{n}}(E)$ can be interpreted as the fraction of the $\bar{n}$th box state lying in the physical continuum of the hydrogen target. The accuracy of this approximation depends on

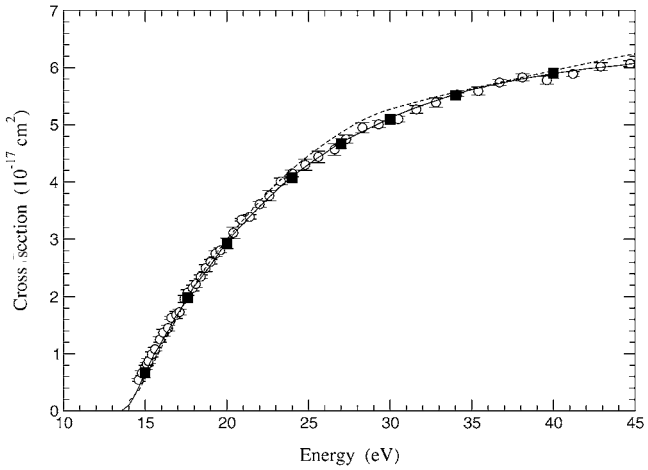

Figure 1. Total cross section for electron-impact ionization of the ground state of hydrogen. Theoretical results: ■, wavepacket propagation; ——, two-electron R-matrix propagation; - - - -, CCC calculation. Experimental results: ○, Shah *et al* 1987.

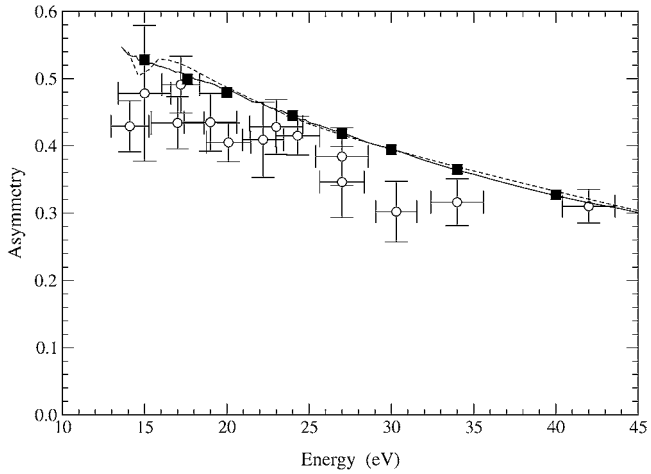

Figure 2. Spin asymmetry for electron-impact ionization of the ground state of hydrogen. Theoretical results: ■, wavepacket propagation; ——, two-electron R-matrix propagation; - - - -, CCC calculation. Experimental results: ○, Fletcher *et al* 1985.

the density of states in the energy range considered, which in turn is a function of the distance of propagation.

The results reported here using this time-independent approach have been obtained by propagating the R-matrix in the two directions r_1, r_2 in steps of 10 a_0 out to a distance of 120 a_0. A total of 250 states and pseudostates of angular momentum $\ell \leqslant 5$ are included in the close-coupling calculation, of which 45 have negative energies. All the $n \leqslant 6$ physical target states are accurately represented. Partial waves up to $L = 19$ are included.

In table 1, we compare the partial ionization cross sections for $L \leqslant 4$ obtained using the two methods described above. The agreement is very good, particularly for $E \geqslant 20$ eV, where the largest relative difference is approximately 4%. At 15 eV, the relative differences do not

Table 1. Partial ionization cross sections (10^{-18} cm^2): WP, wavepacket propagation; RM, two-electron R-matrix propagation; CCC, convergent close-coupling calculation; TDCC, time-dependent close-coupling calculation (Pindzola and Schultz 1996).

Symmetry		15 eV	20 eV	30 eV	40 eV
^{1}S	WP	0.79	2.57	2.93	2.44
	RM	0.80	2.64	2.97	2.44
	CCC		2.72	2.91	2.53
	TDCC		2.17	2.90	2.57
^{3}S	WP	0.003	0.07	0.32	0.47
	RM	0.001	0.07	0.33	0.48
	CCC		0.06	0.33	0.50
	TDCC		0.09	0.33	0.53
^{1}P^o	WP	0.85	3.53	4.93	4.50
	RM	0.86	3.59	4.97	4.53
	CCC			5.04	4.41
	TDCC			4.07	3.94
^{3}P^o	WP	0.65	1.67	1.65	1.52
	RM	0.69	1.73	1.66	1.53
	CCC			1.65	1.51
	TDCC			1.56	1.46
^{1}D	WP	2.23	7.74	9.00	7.51
	RM	2.27	7.94	9.09	7.48
^{3}D	WP	0.37	1.91	3.17	3.33
	RM	0.37	1.94	3.21	3.36
^{1}F^o	WP	0.27	2.41	5.28	5.73
	RM	0.25	2.36	5.30	5.73
^{3}F^o	WP	1.13	4.64	6.32	5.99
	RM	1.15	4.69	6.34	6.06
^{1}G	WP	0.14	1.06	2.77	3.59
	RM	0.13	1.02	2.75	3.62
^{3}G	WP	0.15	1.91	4.97	5.88
	RM	0.13	1.85	5.00	5.94
⋮					
Total	WP	6.66	29.30	50.99	59.02
	RM	6.73	29.48	51.13	58.97

exceed 16% except for the ^{3}S partial wave whose contribution is, however, particularly small. The relative difference in the total cross section is always less than 1%. For the partial waves $L = 0$ and 1, there is also good agreement with the results of a convergent close-coupling (CCC) calculation (Bray and Stelbovics (1992), cited by Pindzola and Schultz (1996)), and those of the TDCC method using a uniform spatial grid out to 40 a_0 (Pindzola and Schultz 1996). For $L = 0$, the TDCC results at 30 and 40 eV lie slightly closer to the CCC results than ours, while at 20 eV the reverse is true. For $L = 1$, our results are in better agreement with the CCC calculation than the TDCC results.

In figure 1, we compare our values for the total cross section with those of experiment (Shah *et al* 1987), as well as with results obtained using the CCC method, taken from the online database at http://atom.murdoch.edu.au/CCC-WWW/index.html. As already indicated in table 1, there is excellent agreement between the results of the wavepacket and two-electron

R-matrix propagation methods. The differences are hardly visible on the scale of figure 1, even at the lowest energies. There is also excellent agreement throughout the whole energy range with the experimental results of Shah *et al* (1987), obtained using a pulsed crossed-beam technique. Most of our values lie within the experimental error bars, which correspond to a 67% confidence level, with an additional uncertainty of 6.8% in the absolute values associated with the normalization procedure. Some small differences with the CCC results can be seen, notably in the region of 30 and 45 eV.

We have also calculated the spin asymmetry parameter

$$A_{\mathrm{I}}(E) = \frac{(\sigma_{\mathrm{I}}^0 - \sigma_{\mathrm{I}}^1/3)}{\sigma_{\mathrm{I}}}$$

where $\sigma_{\mathrm{I}}^0, \sigma_{\mathrm{I}}^1$ are the singlet and triplet ionization cross sections, respectively. Our results are presented in figure 2, together with those of the CCC calculation and the experiment of Fletcher *et al* (1985). Once again there is generally very good agreement between the three sets of theoretical results, although some small differences occur at lower collision energies. The CCC curve has a small dip near 15 eV, which is not visible in the results of the other two calculations, nor in those of an R-matrix with pseudostates calculation (Bartschat and Bray 1996). The tiny structures seen in the RM curve below 25 eV are due to pseudoresonances. All three theoretical curves lie slightly above the experimental results.

We have shown that the wavepacket and R-matrix propagation methods give accurate values of total ionization cross sections and asymmetry parameters in the intermediate energy region between 15 and 40 eV. In the wavepacket approach, the non-uniform grid generated by the Coulomb reference function is well adapted and efficient for describing collisional processes. In particular, a large portion of configuration space can be spanned with a reasonable number of points. The efficiency of this representation allows us to apply the wavepacket propagation method for all partial waves until convergence is achieved, even at relatively low collision energy. We are currently extending our calculations in order to obtain differential ionization cross sections.

The wavepacket calculations were performed at the Pôle de Calcul Intensif de l'Ouest, Université de Rennes 1, on computers financed by the Conseil Régional de Bretagne and the Ministère de l'Education Nationale, de la Recherche et de la Technologie, and at the Institut du Développement et des Ressources en Informatique Scientifique (IDRIS), Orsay, France (project 021311). Calculations using the two-electron R-matrix propagator were performed at the Centre Informatique National de l'Enseignement Supérieur (CINES), France (project LSA 2538).

References

Bartschat K and Bray I 1996 *J. Phys. B: At. Mol. Opt. Phys.* **29** L577
Bottcher C 1981 *J. Phys. B: At. Mol. Phys.* **14** L349
Bray I and Stelbovics A T 1992 *Phys. Rev.* A **46** 6995
Colgan J, Pindzola M S, Robicheaux F J, Griffin D C and Baertschy M 2002 *Phys. Rev.* A **65** 042721
Dunseath K M, Launay J-M, Terao-Dunseath M and Mouret L 2002 *J. Phys. B: At. Mol. Opt. Phys.* **35** 3539
Dunseath K M, Le Dourneuf M, Terao-Dunseath M and Launay J-M 1996 *Phys. Rev.* A **54** 561
Feit M D, Fleck J R and Steiger A 1982 *J. Chem. Phys.* **47** 412
Fletcher G D, Alguard M J, Gay T J, Wainwright P F, Lubell M S, Raith W and Hughes V W 1985 *Phys. Rev.* A **31** 2854
Gallaher D F 1974 *J. Phys. B: At. Mol. Phys.* **7** 362
Ihra W, Draeger M, Handke G and Friedrich H 1995 *Phys. Rev.* A **52** 3752
Percival I C and Seaton M J 1957 *Proc. Camb. Phil. Soc.* **53** 654

Pindzola M S, Colgan J, Robicheaux F and Griffin D C 2000 *Phys. Rev.* A **62** 042705
Pindzola M S and Robicheaux F 1996 *Phys. Rev.* A **54** 2142
Pindzola M S and Robicheaux F 2000 *J. Phys. B: At. Mol. Opt. Phys.* **33** L427
Pindzola M S and Schultz D R 1996 *Phys. Rev.* A **53** 1525
Schwartz C 1985 *J. Math. Phys.* **26** 411
Shah M B, Elliott D S and Gilbody H B 1987 *J. Phys. B: At. Mol. Phys.* **20** 3501